"Smart" Rotaxanes: Shape Memory and Control in Tertiary Amide Peptido[2]rotaxanes

William Clegg,[†] **Carlos Gimenez-Saiz,**[‡] **David A. Leigh,**[*,§] **Aden Murphy,**[§]
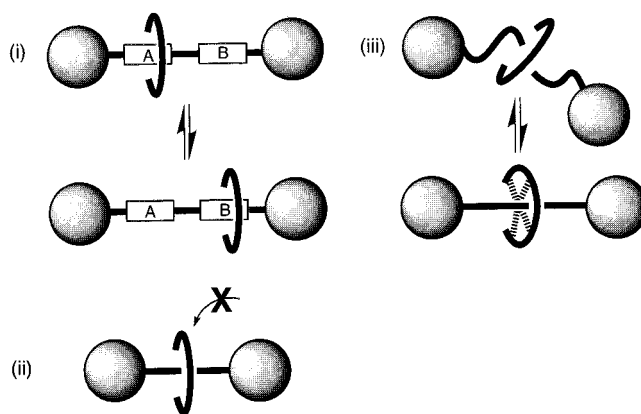**Alexandra M. Z. Slawin,**[‡] **and Simon J. Teat**[†]

*Contribution from the Centre for Supramolecular and Macromolecular Chemistry,
Department of Chemistry, University of Warwick, Coventry CV4 7AL, United Kingdom,
the Molecular Structure Laboratory, Department of Chemistry, University of Loughborough, United
Kingdom, the Department of Chemistry, University of Newcastle, Newcastle-upon-Tyne, United Kingdom,
and the CCLRC Daresbury Laboratory, Warrington, United Kingdom*

Received November 30, 1998. Revised Manuscript Received March 11, 1999

Abstract: The structures of the first tertiary amide peptide rotaxanes are established in solution by ^{1}H NMR spectroscopy and in the solid state by *X*-ray crystallography. The hydrogen bonding networks which template the rotaxane formation "live on" in nonpolar solvents and strongly influence either the tertiary amide rotamer distribution or the rate of interconversion between the rotamers depending upon the peptide sequence. The intercomponent interactions—and their influences—can in appropriate cases be "switched off" by polar solvents leading to "smart" molecular systems which are flexible or adopt several shapes in one environment but transformed to rigid or single-shaped species in another.

Introduction

Interest in the properties of rotaxanes[1] (where a macrocycle is mechanically locked onto a linear thread by bulky stoppers, Figure 1) has thus far largely focused on (i) translational isomerism (changing the distance or orientation between parts of the interlocked components with a view to developing "molecular machinery")[2] and (ii) the isolation of sections of the thread from the outside world[3] (leading to dramatic changes in properties such as solubility,[3a−c] aggregation,[3c] biocompatability,[3d,e] crystallinity,[1c,3a,f] fluorescence,[3g] electrochemistry,[3h] and

* Address correspondence to this author. E-mail: David.Leigh@Warwick. ac.uk.
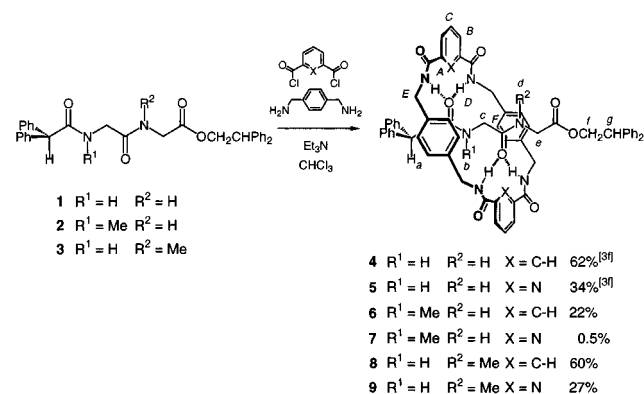† University of Newcastle and CCLRC Daresbury.
‡ University of Loughborough.
§ University of Warwick.

(1) (a) Schill, G. *Catenanes, Rotaxanes and Knots*; Academic Press: New York, 1971. (b) Chambron, J.-C.; Dietrich-Buchecker, C. O.; Sauvage, J.-P. *Top. Curr. Chem.* **1993**, *165*, 131−162. (c) Gibson, H. W.; Bheda, M. C.; Engen, P. T. *Prog. Polym. Sci.* **1994**, *19*, 843−945. (d) Amabilino, D. B.; Stoddart, J. F. *Chem. Rev.* **1995**, *95*, 2725−2828. (e) Leigh, D. A.; Murphy, A. *Chem. Ind.* **1999**, 178−183.
(2) (a) Anelli, P.-L.; Spencer, N.; Stoddart, J. F. *J. Am. Chem. Soc.* **1991**, *113*, 5131−5133. (b) Ashton, P. R.; Bissell, R. A.; Spencer, N.; Stoddart, J. F.; Tolley, M. S. *Synlett* **1992**, 914−918. (c) Ashton, P. R.; Bissell, R. A.; Górski, R.; Philp, D.; Spencer, N.; Stoddart, J. F.; Tolley, M. S. *Synlett* **1992**, 919−922. (d) Ashton, P. R.; Bissell, R. A.; Spencer, N.; Stoddart, J. F.; Tolley, M. S. *Synlett* **1992**, 923−926. (e) Bissell, R. A.; Córdova, E.; Kaifer, A. E.; Stoddart, J. F. *Nature* **1994**, *369*, 133−137. (f) Benniston, A. C.; Harriman, A.; Lynch, V. M. *J. Am. Chem. Soc.* **1995**, *117*, 5275−5291. (g) Benniston, A. C. *Chem. Soc. Rev.* **1996**, *25*, 427−435. (h) Collin, J.-P.; Gaviña, P.; Sauvage, J.-P. *Chem. Commun.* **1996**, 2005−2006. (i) Ashton, P. R.; Ballardini, R.; Balzani, V.; Boyd, S. E.; Credi, A.; Gandolfi, M. T.; Gómez-López, M.; Iqbal, S.; Philp, D.; Preece, J. A.; Prodi, L.; Ricketts, H. G.; Stoddart, J. F.; Tolley, M. S.; Venturi, M.; White, A. J. P.; Williams, D. J. *Chem. Eur. J.* **1997**, *3*, 152−170. (j) Anelli, P.-L.; Asakawa, M.; Ashton, P. R.; Bissell, R. A.; Clavier, G.; Górski, R.; Kaifer, A. E.; Langford, S. J.; Mattersteig, G.; Menzer, S.; Philp, D.; Slawin, A. M. Z.; Spencer, N.; Stoddart, J. F.; Tolley, M. S.; Williams, D. J. *Chem. Eur. J.* **1997**, *3*, 1113−1135. (k) Lane, A. S.; Leigh, D. A.; Murphy, A. *J. Am. Chem. Soc.* **1997**, *119*, 11092−11093. (l) Murakami, H.; Kawabuchi, A.; Kotoo, K.; Kunitake, M.; Nakashima, N. *J. Am. Chem. Soc.* **1997**, *119*, 7605−7606. (m) Gong, C.; Glass, T. E.; Gibson H. W. *Macromolecules* **1998**, *31*, 308−313. (n) Balzani, V.; Gómez-López, M.; Stoddart, J. F. *Acc. Chem. Res.* **1998**, *31*, 405−414.

Figure 1. Properties of rotaxane architectures: (i) variable separation of pendant functionality on thread and macrocycle; (ii) changing the nature of interaction between the thread and the outside world (protection by encapsulation, solubility changes etc.); and (iii) changing shape through switchable thread−macrocycle interactions.

stability[3f]). Here we describe a new type of phenomenon as a result of mechanical bonding, where the conformation adopted by one of the mechanically interlocked components is regulated through selectively activated noncovalent interactions with another.[4] In these tertiary amide peptido[2]rotaxanes the macrocycle "remembers" or "forgets" the intercomponent amide hydrogen bonding motif originally responsible for rotaxane formation according to the nature of its environment. The intramolecular interactions govern the kinetics and/or thermo-

(3) (a) Gibson, H. W.; Liu, S.; Lecavalier, P.; Wu, C.; Shen, Y. X. *J. Am. Chem. Soc.* **1995**, *117*, 852−874 and references therein. (b) Johnston, A. G.; Leigh, D. A.; Murphy, A.; Smart, J. P.; Deegan, M. D. *J. Am. Chem. Soc.* **1996**, *118*, 10662−10663. (c) Anderson, S.; Claridge, T. D. W.; Anderson, H. L. *Angew. Chem., Int. Ed. Engl.* **1997**, *36*, 1310−1313. (d) Ooya, T.; Yui, N. J. *Biomater. Sci. Polym.* **1998**, *8*, 437−455. (e) Yui, N.; Ooya, T.; Kumeno, T. *Bioconj. Chem.* **1998**, *9*, 118−125. (f) Leigh, D. A.; Murphy, A.; Smart, J. P.; Slawin, A. M. Z. *Angew. Chem., Int. Ed. Engl.* **1997**, *36*, 728−731. (g) Anderson, S.; Anderson, H. L. *Angew. Chem., Int. Ed. Engl.* **1996**, *35*, 1956−1959. (h) Córdova, E.; Bissell, R. A.; Kaifer, A. E. *J. Org. Chem.* **1995**, *60*, 1033−1038.

Scheme 1. Synthesis of the Peptido[2]rotaxanes **4**−**9**[a]

1 R[1] = H R[2] = H
2 R[1] = Me R[2] = H
3 R[1] = H R[2] = Me

4 R[1] = H	R[2] = H	X = C-H	62%[3f]
5 R[1] = H	R[2] = H	X = N	34%[3f]
6 R[1] = Me	R[2] = H	X = C-H	22%
7 R[1] = Me	R[2] = H	X = N	0.5%
8 R[1] = H	R[2] = Me	X = C-H	60%
9 R[1] = H	R[2] = Me	X = N	27%

[a] Threads **2** and **3** were prepared from the corresponding *N*-terminus aminoacid methyl ester: (i) Ph$_2$CHCOCl, Et$_3$N, CHCl$_3$; (ii) NaOH, EtOH; (iii) *N*-hydroxysuccinimide, DCC, THF, 0 °C; (iv) *C*-terminus aminoacid methyl ester, Et$_3$N, CHCl$_3$; (v) Ph$_2$CHCH$_2$OH, (Bu$_2$SnCl)$_2$O, PhMe, Δ. Overall yields: **2**, 73%; **3**, 78%.

dynamics of the equilibrium between the tertiary amide group rotamers[5] in the backbone of the thread which, in turn, strongly influence the overall shape of the molecule.[6] Thus "smart" mechanically interlocked molecules can be designed that are flexible or adopt several shapes in polar media (where the intercomponent H-bonding is broken by the competing solvent) but reversibly transformed to more rigid or single-shaped species in nonpolar solvents and the solid state.[7]

Results and Discussion

We recently described[3f] the hydrogen bond-mediated synthesis of rotaxanes **4** and **5** from the glycylglycine-based dipeptide thread, **1**.[8] As part of an investigation into the structural tolerance of this reaction we prepared rotaxanes **6**−**9** with sarcosine (*N*-methylglycine) substituted for one or the other of the glycine residues in the thread (Scheme 1). Although yields of the glycylsarcosine-based rotaxanes (**8** and **9**) were similar to those obtained using the glycylglycine thread, the yields of rotaxanes **6** and **7** (using the sarcosylglycine thread) were much lower, suggesting that derivatization close to the key hydrogen bonding sites of the thread sterically hinders the complementary fit between the thread and the precursor to macrocyclization,

(4) For examples of rotaxanes where intramolecular interactions bring about changes in the photochemical and/or electrochemical behavior of the individual components see ref 2g or: Amabilino, D. B.; Ashton, P. R.; Balzani, V.; Brown, C. L.; Credi, A.; Fréchet, J. M. J.; Leon, J. W.; Raymo, F. M.; Spencer, N.; Stoddart, J. F.; Venturi, M. *J. Am. Chem. Soc.* **1996**, *118*, 12012−12020 and references therein.

(5) For hydrogen bond-assembled host−guest complexes which stabilize a particular secondary amide bond rotamer see: (a) Vicent, C.; Hirst, S. C.; Garcia-Tellado, F.; Hamilton, A. D. *J. Am. Chem. Soc.* **1991**, *113*, 5466−5467. (b) Pernía, G. J.; Kilburn, J. D.; Essex, J. W.; Mortishire-Smith, R. J.; Rowley, M. *J. Am. Chem. Soc.* **1996**, *118*, 10220−10227. (c) Moraczewski, A. L.; Banaszynski, L. A.; From, A. M.; White, C. E.; Smith, B. D. *J. Org. Chem.* **1998**, *63*, 7258−7262.

(6) For control over the shape of macromolecules with flexible backbones through intramolecular interactions see: Percec, V.; Ahn, C.-H.; Ungar, G.; Yeardley, D. J. P.; Möller, M.; Sheiko, S. S. *Nature* **1998**, *391*, 161−164.

(7) For a comprehensive account of smart materials with a recoverable inherent or predetermined shape, function, or property see: *Shape Memory Materials*; Otsuka, K., Wayman, C. M., Eds.; Cambridge University Press: Cambridge, 1998. For other conformationally switchable molecules which respond to changes in their environment see: (a) Höger, S.; Enkelmann, V. *Angew. Chem., Int. Ed. Engl.* **1995**, *34*, 2713−2716. (b) Höger, S.; Meckenstock, A. D.; Muller, S. *Chem. Eur. J.* **1998**, *4*, 2423−2434. (c) Leigh, D. A.; Moody, K.; Smart, J. P.; Watson, K. J.; Slawin, A. M. Z. *Angew. Chem., Int. Ed. Engl.* **1996**, *35*, 306−310. (d) Janout, V.; Lanier, M.; Regen, S. L. *J. Am. Chem. Soc.* **1996**, *118*, 1573−1574. (e) Janout, V.; Lanier, M.; Regen, S. L. *J. Am. Chem. Soc.* **1997**, *119*, 640−647.
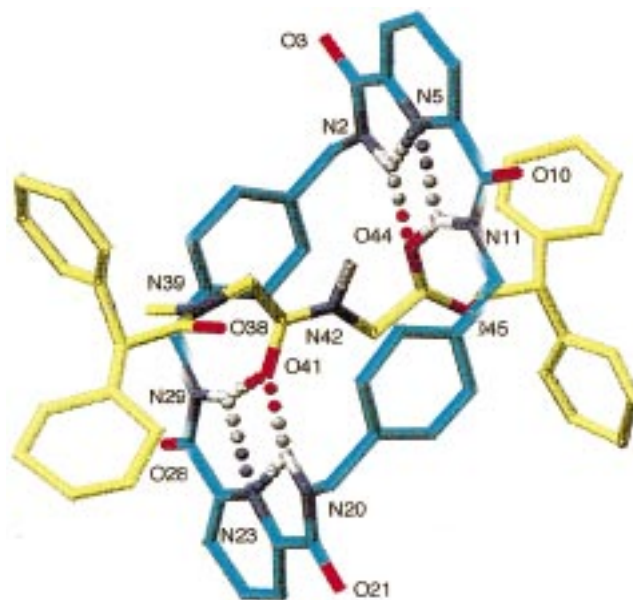

Figure 2. Solid-state structure of the sarcosylglycine peptido[2]-rotaxane (**7**) as determined by X-ray crystallography (for clarity carbon atoms of the macrocyclic ring are shown in blue and the carbon atoms of the thread in yellow; oxygen atoms are depicted in red, nitrogen atoms dark blue, and hydrogen atoms white). In the crystal lattice the macrocycles form layers in the [1 0 −1] plane such that each forms pyridine ring−xylylene ring π−π stacking interactions with the four nearest neighboring macrocycles.

thus reducing the efficiency of rotaxane formation. This was particularly significant in the case of the 2,6-diamidopyridyl-derived rotaxane, **7**, which could only be isolated in 0.5% yield.[9] The synchrotron-source X-ray structure (Figure 2) of small crystals grown by slow evaporation from ethanol shows that, in marked contrast to other dipeptide rotaxanes, the macrocycle of **7** is not located primarily around the *N*-terminal (in this case, sarcosine) amino acid unit but around the *C*-terminus (glycine) residue. In the solid state the *N*-methyl amide group (O38−N39) is twisted orthogonally to the rest of the peptide backbone which only permits the macrocycle to hydrogen bond to one amide group (O41) of the thread with the other amides of the macrocycle having to be satisfied by the much poorer H-bond-accepting ester carbonyl (O44).

The other tertiary amide peptide rotaxanes (**6**, **8**, and **9**) adopt more conventional component co-conformations,[10] as evidenced by shifts in their ^{1}H NMR spectra (Figures 3, 5, and 6), with the macrocycle encapsulating the *N*-terminus amino acid residue and central portion of the thread in C$_2$D$_2$Cl$_4$ utilizing hydrogen bonding motifs which bridge the two peptide amide groups. However, the three rotaxanes display behavior differing from one another in terms of both the populations (i.e., thermodynamics) of and rotational energy barriers (i.e., kinetics) between their *Z* and *E* tertiary amide rotamers in solution—a significant factor in determining the overall shape of the thread (Figures 4 and 7).

The *Z* and *E* rotamers of the tertiary amides of the threads in these systems are of roughly similar stabilities and, because of the partial double bond character of the C−N bond, interconvert only slowly at room temperature leading to both rotamers being evident via ^{1}H NMR spectroscopy.[11] The ^{1}H NMR spectra of the sarcosylglycine thread **2** in C$_2$D$_2$Cl$_4$ is shown in Figure 3a. ROESY[12] experiments confirm that the *N*-methyl group (H$_b$) is *E* to the carbonyl oxygen in the major rotamer, minimizing unfavorable interactions with the *N*-terminus diphenylmethine
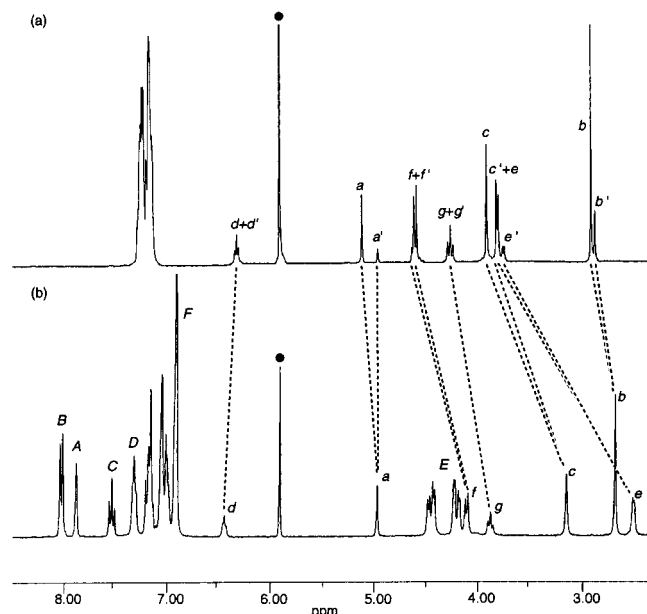
Figure 3. ^{1}H NMR spectra (300 MHz) of (a) the sarcosylglycine thread (**2**) and (b) the isophthaloyl macrocycle-containing sarcosylglycine rotaxane (**6**) in C$_2$D$_2$Cl$_4$ (• = residual solvent). Resonances attributable to the minor, *Z*, rotamer are labeled with a prime.
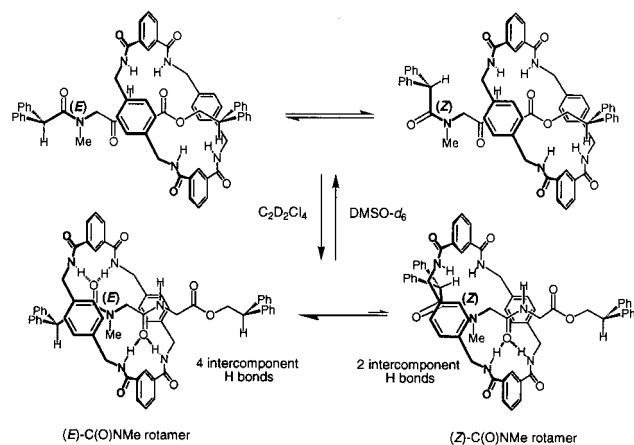

Figure 4. Conformational isomerism of the peptide in the isophthaloyl macrocycle-containing sarcosylglycine rotaxane (**6**). In C$_2$D$_2$Cl$_4$, hydrogen bonding between macrocycle and thread leads to stabilization of the *E* rotamer over the *Z* rotamer. In DMSO-d_6, the intramolecular hydrogen bonding is switched off and both rotamers are observed by NMR.

stopper.[13] Two tertiary amide rotamers are also apparent in the room temperature ^{1}H NMR spectra of the glycylsarcosine thread (**3**) and rotaxanes (**8** and **9**) in both C$_2$D$_2$Cl$_4$ (Figure 6, parts a, b and c, respectively) and DMSO-d_6. Remarkably, however, for the isophthaloyl macrocycle-derived sarcosylglycine rotaxane (**6**) only a single tertiary amide rotamer (again shown to be *E*

(8) For other amide-based rotaxanes see: Vögtle, F.; Dünnwald, T.; Schmidt T. *Acc. Chem. Res.* **1996**, *29*, 451−460.

(9) The preference of pyridine-2,6-dicarbamido units for a syn conformation with two intramolecular NH···N(pyr) hydrogen bonds is now well established [Newkome, G. R.; Fronczek, F. R.; Kohli, D. K. *Acta Crystallogr.* **1981**, *B37*, 2114−2117. Hunter, C. A.; Purvis, D. H. *Angew. Chem., Int. Ed. Engl.* **1992**, *31*, 792−795. Johnston, A. G.; Leigh, D. A.; Nezhat, L.; Smart, J. P.; Deegan, M. D. *Angew. Chem., Int. Ed. Engl.* **1995**, *34*, 1212−1216. Hamuro, Y.; Geib, S. J.; Hamilton, A. D. *J. Am. Chem. Soc.* **1997**, *119*, 10587−10593]. This reduces the number of low-energy conformations available to the macrocycle and, in particular, dramatically increases the energy required to make the kind of out-of-plane distortions required of the aromatic dicarbonyl system to accommodate steric hindrances around the hydrogen bonding template sites.
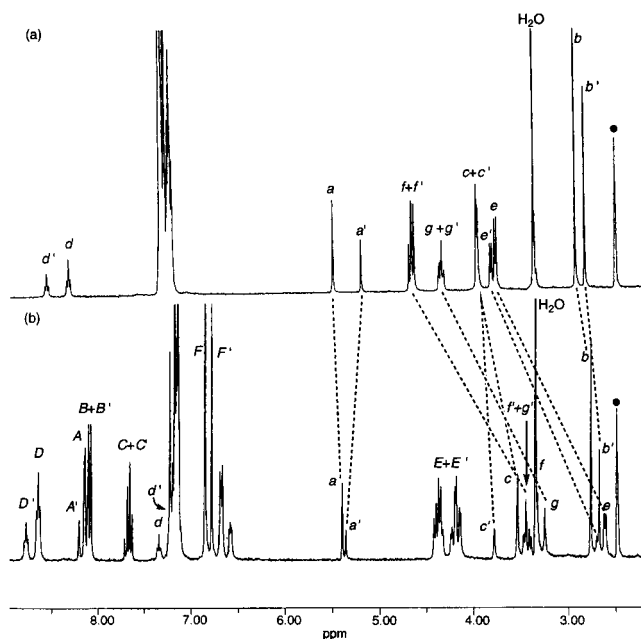

Figure 5. ^{1}H NMR spectra (300 MHz) of (a) the sarcosylglycine thread (**2**) and (b) the isophthaloyl macrocycle-containing sarcosylglycine rotaxane (**6**) in DMSO-d_6.
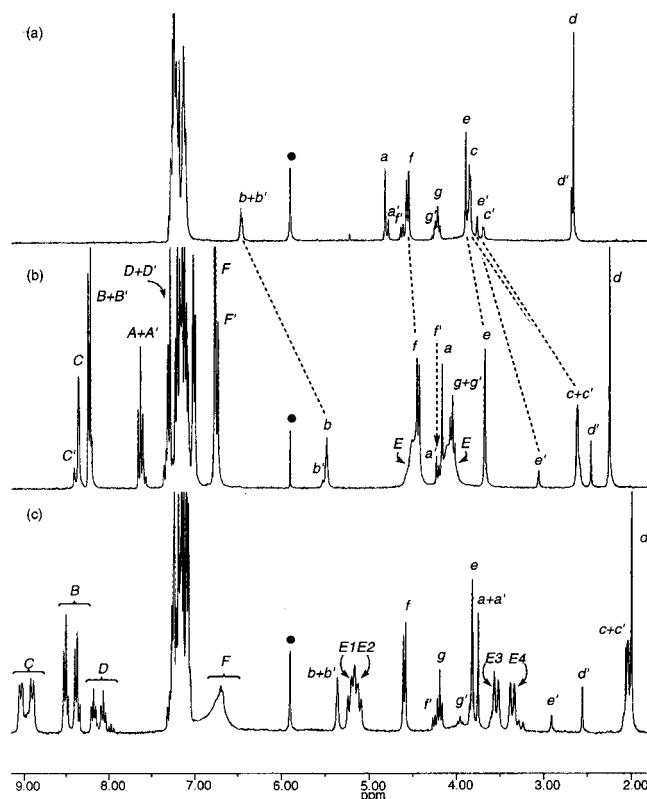
Figure 6. ^{1}H NMR spectra (300 MHz) of (a) the glycylsarcosine thread (**3**), (b) the isophthaloyl macrocycle-containing glycylsarcosine rotaxane (**8**), and (c) the pyridyl macrocycle-containing glycylsarcosine rotaxane (**9**) in C$_2$D$_2$Cl$_4$.

by ROESY experiments) is observed in C$_2$D$_2$Cl$_4$ by ^{1}H NMR (Figure 3b). Most protons of the peptide portion of **6** are shielded by the macrocycle aromatic rings, with the greatest shifts being for H$_c$ and H$_e$, locating the macrocycle over the glycine unit and central portion of the thread. A notable exception is the glycyl amide proton, H$_d$, which is deshielded due to hydrogen bonding with the amide carbonyls of the macrocycle in some
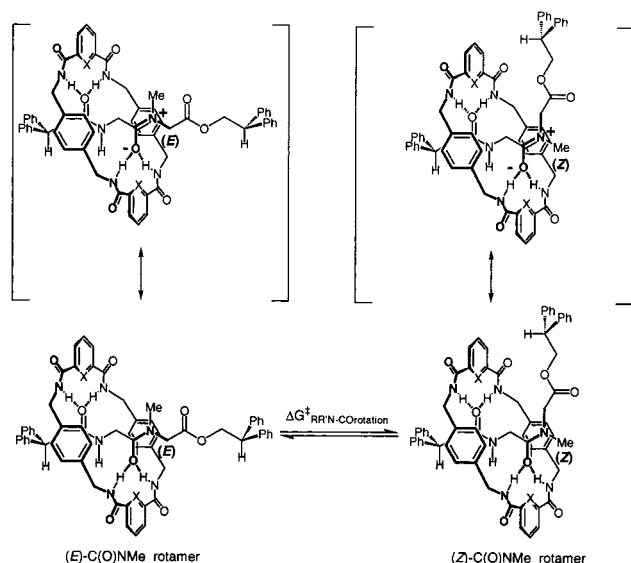
Figure 7. Solution structures of the glycylsarcosine rotaxanes **8** and **9**. The contributions of the zwitterionic resonance forms are largely responsible for the observed restricted rotation about the tertiary amide bond. Stabilization of the zwitterion via intramolecular hydrogen bonding (in $C_2D_2Cl_4$ for **8**; in both $C_2D_2Cl_4$ and DMSO-d_6 for **9**) increases the energy barrier to rotation compared to that of the thread (**3**) alone.

Table 1. Rotational Energy Barriers (± 0.1 kcal mol^{-1}) and Frequencies of Rotation ($\pm 10\%$) for the Tertiary Amide C(O)−NMe Bond at 298 K As Determined by SPT-SIR[18] of the Sarcosyl Methylene Group (H$_{e/e'}$) Resonances

	rotational energy barrier/kcal mol^{-1} (freq of rotation/Hz)	
	$C_2D_2Cl_4$	DMSO-d_6
glycylsarcosine thread **3**	18.3 (0.2)	18.0 (0.4)
isophthaloyl rotaxane **8**	20.2 (0.009)	18.1 (0.3)
pyridyl rotaxane **9**	21.6 (0.0009)	21.2 (0.002)

of the intercomponent hydrogen bonding motifs that can be adopted.[14] Molecular modeling reveals several low-energy co-conformations for the C(O)N−Me *E* rotamer of **6** that allow four hydrogen bonds to be formed between macrocycle and thread compared with only two in the *Z* rotamer (Figure 4). This additional stabilization lowers the energy of the *E* rotamer to such an extent (4−6 kcal mol^{-1}) that the *Z* rotamer is no longer detected by ^{1}H NMR spectroscopy.[15] The selection of one rotamer over the other through hydrogen bond stabilization is all the more remarkable given the dynamic nature of the intercomponent hydrogen bonding; the simplicity in appearance of the macrocycle resonances (H$_{A−F}$) indicates that the macrocycle spins rapidly about the thread at room temperature although this requires momentary breaking of all four intercomponent hydrogen bonds which control the tertiary amide conformation.

In DMSO-d_6, the hydrogen bonding between the peptide and macrocycle in **6** is broken, and the enhanced relative shielding of protons H$_{e/e'}$ and H$_{g/g'}$ indicates that the macrocycle spends

more time over the *C*-terminus amino acid of the thread (Figure 5b). Most significantly, by switching off the hydrogen bonding between macrocycle and thread the *E* rotamer is no longer stabilized and a mixture of two rotamers is reestablished!

While NMR shifts indicate the intercomponent hydrogen bonding motifs adopted by the glycylsarcosine rotaxanes (**8** and **9**) are similar to that found for **6**, the effect that the macrocycle has upon the thread is markedly different. The ^{1}H NMR spectra of the thread (**3**) and rotaxane (**8**) in $C_2D_2Cl_4$ are shown in Figures 6a and 6b. In contrast to **6** both *Z* and *E* tertiary amide rotamers of the thread can now form four hydrogen bonds to the macrocycle (Figure 7); correspondingly, both rotamers are observed by NMR in both polar and nonpolar solvents. As in **6**, protons located within the macrocyclic cavity (e.g., H$_c$ and H$_{c'}$) experience the largest (> 1.3 ppm) upfield shifts whereas protons situated outside the cavity (such as H$_f$) experience little or no shielding at all. Interestingly, protons H$_{e'}$ and H$_{f'}$ in the minor, *Z*, rotamer are considerably more shielded than the analogous resonances in the major, *E*, rotamer with the twisting about the tertiary amide bond placing them directly over an isophthaloyl aromatic ring (Figure 7). In contrast, H$_{d'}$ in the *Z* rotamer is moved away from the same aromatic ring and is thus de-shielded relative to H$_d$ of the *E* rotamer. Pirouetting of the pyridyl macrocycle about the glycylsarcosine thread is slowed[16] with respect to the analogous glycylglycine rotaxane (**5**),[3f] giving rise to four distinct signals for the eight H$_E$ protons (resonances H$_{E1−4}$, the backbone of the thread is effectively a plane of symmetry, Figure 6c). In DMSO-d_6, as with the glycylglycine rotaxanes,[3f] hydrogen bonding between the macrocycle and thread is broken in the case of the isophthaloyl-derived macrocycle (rotaxane **8**), but maintained with the pyridyl one (rotaxane **9**).

While the macrocycle can no longer significantly alter the preferred conformation of the thread in rotaxanes **8** and **9** (since the number of intercomponent hydrogen bonds is the same for both tertiary amide rotamers), it still exerts a profound influence upon it. Table 1 shows the activation energies[17] for rotation about the tertiary amide C−N bond in the glycylsarcosine-based thread and rotaxanes in $C_2D_2Cl_4$ and DMSO-d_6 as determined through spin polarization transfer by selective inversion recovery (SPT-SIR[18]) experiments. Restricted rotation about the amide bond is a consequence of the partial double bond character contributed by the $^-$O−C=N$^+$ resonance form (Figure 7). Intercomponent hydrogen bonding in **8** and **9** stabilizes negative polarization of the oxygen atom, increasing the contribution of the zwitterionic form to the overall structure, thus increasing the activation energy for bond rotation and slowing down rotamer interconversion. In $C_2D_2Cl_4$ the increase in $\Delta G^{\ddagger}_{RR'N−COrot^n}$

(10) "Co-conformation" refers to the relative positions and orientations of the mechanically interlocked components with respect to each other [Fyfe, M. C. T.; Glink, P. T.; Menzer, S.; Stoddart, J. F.; White, A. J. P.; Williams, D. J. *Angew. Chem., Int. Ed. Engl.* **1997**, *36*, 2068−2069].

(11) (a) Stewart, W. E.; Siddall, T. H., III *Chem. Rev.* **1970**, *70*, 517−551. (b) Thomas, W. A.; Williams, M. K. *J. Chem. Soc., Chem. Commun.* **1972**, 788−789.

(12) The *E*-stereochemistry of the major rotamer was unambiguously determined by the presence of an nOe between resonances H$_a$ and H$_b$ in ROESY experiments. Similarly, in the minor, *Z*, isomer a strong enhancement was observed between H$_{b'}$ and H$_{c'}$.

(13) This is consistent with conformational studies on other tertiary amides, e.g.: LaPlanche, L. A.; Rogers, M. T. *J. Am. Chem. Soc.* **1963**, *85*, 3728−3730. The major rotamers observed in all the threads and rotaxanes reported here were found to be *E* by ROESY experiments.

(14) The extent of deshielding is much less than that for the same proton in the glycylglycine system [ref 3f], suggesting a greater population of macrocycle conformations with all four amide carbonyls exo to the cavity.

(15) For other examples of the stabilization of tertiary amide rotamers by intramolecular hydrogen bonding see: (a) Madison, V.; Atreyi, M.; Deber, C. M.; Blout, E. R. *J. Am. Chem. Soc.* **1974**, *96*, 6725−6734. (b) Tamaki, M.; Komiya, S.; Yabu, M.; Watanabe, E.; Akabori, S.; Muramatsu, I. *J. Chem. Soc., Perkin Trans. 1* **1997**, 3497−3500.

(16) Pirouetting of the macrocycle in **9** occurs at 1 s^{-1} at 298 K [refs 17 and 18]. The other rotaxanes are not soluble below the coalescence temperatures of the exchange phenomena.

(17) Calculated from the coalescence temperature using a modified Eyring equation [Shanan-Atidi, H.; Bari-Eli, K. H. *J. Phys. Chem.* **1970**, *74*, 961−963].
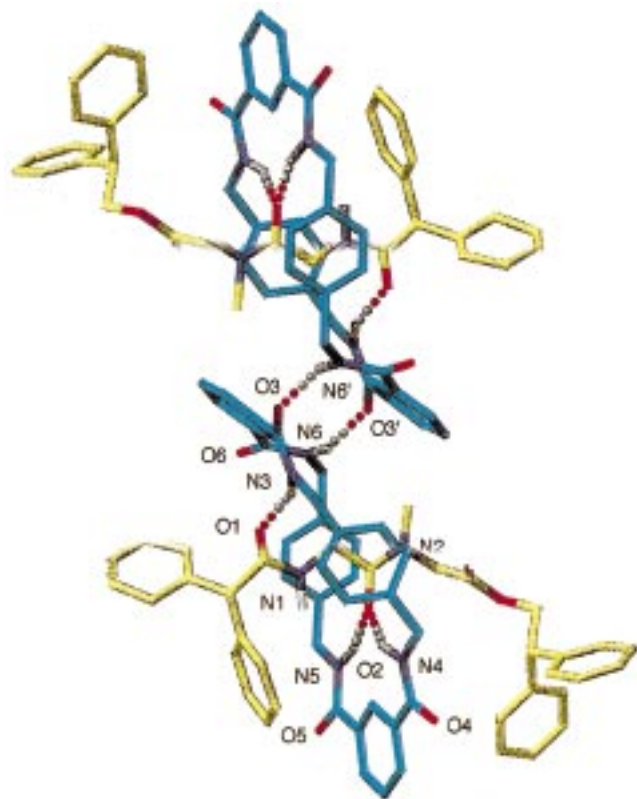
Figure 8. Solid-state structure of the glycylsarcosine peptido[2]-rotaxane (**8**) as determined by X-ray crystallography. Intramolecular hydrogen bond distances (Å): O2−HN4 2.13, O2−HN5 2.06, O1−HN3 1.80. Intermolecular hydrogen bond distances (Å): O3′-HN6 1.97.

for **8** relative to the thread, **3**, is 1.9 kcal mol^{-1}, corresponding to a 100-fold decrease in the rate of rotamer interconversion at 298 K. DMSO-d_6 disrupts the intramolecular hydrogen bonding in **8** and the energy barrier to rotation is restored virtually to that found for **3** (18.1 cf. 18.0 kcal mol^{-1}), showing that this is indeed primarily caused by intercomponent hydrogen bonding and is not just a steric effect.[19] As expected, the phenomenon is essentially solvent-insensitive in the case of the pyridyl rotaxane, **9**, with the barrier to rotation increased by 3.3 kcal mol^{-1} in $C_2D_2Cl_4$ and 3.2 kcal mol^{-1} in DMSO-d_6.

Small single crystals of **8** suitable for investigation by X-ray crystallography using a synchrotron source were obtained by slow evaporation of a solution of the peptido[2]rotaxane in ethanol. The solid state structure (Figure 8) is broadly consistent with that observed for the major co-conformer in $C_2D_2Cl_4$, with the macrocycle located over the *N*-terminal amino acid of the thread. Three hydrogen bonds are present between the macrocycle and the two amide carbonyl groups of the peptide, including an example of the familiar bifurcated hydrogen bonding motif displayed by similar hydrogen bond-assembled systems.[7c,20] The fourth amide group of the macrocycle,

(18) For an account of the SPT-SIR technique applied to catenane architectures see: (a) Leigh, D. A.; Murphy, A.; Smart, J. P.; Deleuze, M. S.; Zerbetto F. *J. Am. Chem. Soc.* **1998**, *120*, 6458−6467. For recent examples of SPT-SIR in other systems see: (b) Ben-David Blanca, M.; Maimon, E.; Kost, D. *Angew. Chem., Int. Ed. Engl.* **1997**, *36*, 2216−2219. (c) Kelly, T. R.; Tellitu, I.; Sestelo, J. P. *Angew. Chem., Int. Ed. Engl.* **1997**, *36*, 1866−1868. (d) Abdourazak, A. H.; Sygula, S.; Rabideau, P. W. *J. Am. Chem. Soc.* **1993**, *115*, 3010−3011. (e) Frim, R.; Zilber, G.; Rabinovitz, M. *J. Chem. Soc. Chem. Commun.* **1991**, 1202−1203. For a review of 2D methods for determining the kinetics of exchange processes see: (f) Perrin, C. L.; Dwyer, T. J. *Chem. Rev.* **1990**, *90*, 935−967.

(19) For steric effects on tertiary amide rotamer equilibria see: Beausoleil, E.; Lubell, W. D. *J. Am. Chem. Soc.* **1996**, *118*, 12902−12908 and references therein.

however, chooses to be involved in intermolecular hydrogen bonding with the macrocycle of an adjacent rotaxane in the solid state.

Conclusions

One of the major issues still to be fully explored in the interlocking of molecular level components is the nature of the physical and chemical effects that can be induced or influenced through such architectures—i.e., what are the benefits and potential applications of the mechanical bond? The rotaxanes reported here exhibit a new and unanticipated type of behavior that could lead to applications in smart materials which are flexible or multi-shaped in one situation (e.g., during processing) but are transformed to rigid or single-shaped species in another (e.g., an end product or device).

Experimental Section

General Method for the Preparation of Benzylic Amide Macrocycle Peptido[2]rotaxanes. The thread **2** or **3** (0.5 g, 0.96 mmol) and triethylamine (1.55 g, 15.4 mmol) were dissolved in anhydrous chloroform (200 mL) and stirred vigorously while solutions of the diamine (7.68 mmol) in anhydrous chloroform (40 mL) and the acid chloride (7.68 mmol) in anhydrous chloroform (40 mL) were simultaneously added over a period of 4 h using motor-driven syringe pumps. The resulting suspension was filtered and concentrated under reduced pressure to afford the crude product which was then washed with ethyl acetate to leave only the unconsumed thread and [2]rotaxane in solution. This mixture was subjected to column chromatography (silica gel, CH$_2$-Cl$_2$/MeOH as eluent) to yield, in order of elution, the unconsumed thread and the peptido[2]rotaxane. Selected data for [2]-(1,7,14,20-tetraaza-2,6,15,19-tetraoxo-3,5,9,12,16,18,22,25-tetrabenzocyclohexacosane)-(diphenylacetylsarcosylglycine 2,2-diphenylethyl ester)-rotaxane (**6**): yield 0.22 g (22%); mp 251 °C; ^{13}C NMR (75 MHz, CDCl$_3$) δ 37.39, 40.45, 44.23, 49.43, 51.70, 54.70, 67.87, 124.32, 127.14, 127.85, 128.44, 128.62, 128.73, 128.95, 129.01, 131.25, 134.21, 137.53, 138.68, 140.22, 166.67, 168.70, 170.16, 173.10; FAB-MS (*m*NBA matrix) *m/z* 1054 [(rotaxane + H)$^+$], 533 [(macrocycle + H)$^+$]. Anal. Calcd for C$_{65}$H$_{60}$N$_6$O$_8$: C 74.1, H 5.7, N 8.0. Found C 74.5, H 5.4, N 7.7. Selected data for [2]-(1,4,7,14,17,20-hexaaza-2,6,15,19-tetraoxo-3,5,9,12,16,18,22,25-tetrabenzocyclohexacosane)-(diphenylacetylsarcosylglycine 2,2-diphenylethyl ester)-rotaxane (**7**): yield 0.005 g (0.5%); mp 219 °C; ^{1}H NMR (300 MHz, CDCl$_3$) δ 2.31 (d, J = 3 Hz, 2 H, H$_e$), 3.08 (s, 3 H, H$_b$), 3.65 (s, 2 H, H$_c$), 4.25 (t, J = 6 Hz, 1 H, H$_g$), 4.42 (br, 8 H, H$_E$), 4.54 (d, J = 6 Hz, 2 H, H$_f$), 5.23 (s, 1 H, H$_a$), 6.88 (s, 8 H, H$_F$), 7.20 (m, 20 H, Ph$_2$CH), 8.16 (t, J = 9 Hz, 2 H, H$_C$), 8.53 (d, J = 9 Hz, 4 H, H$_B$), 8.62 (t, J = 3 Hz, 4 H, H$_D$); ^{13}C NMR (75 MHz, CDCl$_3$) δ 38.53, 42.81, 43.00, 49.62, 51.34, 55.08, 70.02, 126.01, 127.63, 128.00, 128.35, 128.90, 129.04, 129.44, 138.72, 139.21, 139.47, 140.66, 164.01, 169.00, 172.45, 173.29; FAB-MS (*m*NBA matrix) *m/z* 1056 [(rotaxane + H)$^+$], 535 [(macrocycle + H)$^+$]. Anal. Calcd for C$_{63}$H$_{58}$N$_8$O$_8$: C 71.7, H 5.5, N 10.6. Found C 71.2, H 5.6, N 10.6. Selected data for [2]-(1,7,14,20-tetraaza-2,6,15,19-tetraoxo-3,5,9,12,16,18,22,25-tetrabenzocyclohexacosane)-(diphenylacetylglycylsarcosine 2,2-diphenylethyl ester)-rotaxane (**8**): yield 0.61 g (60%); mp 235 °C; ^{13}C NMR (75 MHz, CDCl$_3$) δ 36.40, 42.92, 44.92, 50.74, 51.02, 59.55, 69.02, 123.82, 128.40, 129.28, 129.35, 129.65, 130.03, 130.30, 131.16, 133.46, 134.97, 138.95, 139.50, 141.47, 154.01, 166.88, 168.50, 170.41, 174.22; FAB-MS (*m*NBA matrix) *m/z* 1054 [(rotaxane + H)$^+$]; 533 [(macrocycle + H)$^+$] Anal. Calcd for C$_{65}$H$_{60}$N$_6$O$_8$: C 74.1, H 5.7, N 8.0. Found C 74.2, H 5.7, N 7.9. Selected data for [2]-(1,4,7,14,17,20-hexaaza-2,6,15,19-tetraoxo-3,5,9,12,16,18,22,25-tetrabenzocyclohexacosane)-(diphenyl-acetylglycylsarcosine 2,2-diphenylethyl ester)-rotaxane (**9**): yield 0.27 g (27%); mp 270 °C; ^{13}C NMR (75 MHz, CDCl$_3$) δ 31.04, 35.55, 43.49, 43.87, 49.84, 51.12, 60.12, 126.89, 128.37, 129.09, 129.32,

(20) (a) Johnston, A. G.; Leigh, D. A.; Pritchard, R. J.; Deegan, M. D. *Angew. Chem., Int. Ed. Engl.* **1995**, *34*, 1209−1212. (b) Ottens-Hildebrandt, S.; Nieger, M.; Rissanen, K.; Rouvinen, J.; Meier, S.; Harder, G.; Vögtle, F. *J. Chem. Soc., Chem. Commun.* **1995**, 777−778. (c) Adams, H.; Carver, F. J.; Hunter, C. A. *J. Chem. Soc., Chem. Commun.* **1995**, 809−810.

129.62, 130.01, 130.13, 139.28, 140.13, 141.62, 149.59 164.49, 168.88, 170.70, 172.38; FAB-MS (*m*NBA matrix) *m/z* 1056 [(rotaxane + H)$^+$], 535 [(macrocycle + H)$^+$] Anal. Calcd for $C_{63}H_{58}N_8O_8$: C 71.7, H 5.5, N 10.6. Found C 71.5, H 5.8, N 10.3.

X-ray Crystallographic Structure Determinations. 7: $C_{63}H_{58}N_8O_8$, $M = 1055.17$, crystal size $0.08 \times 0.1 \times 0.18$ mm, monoclinic $P2_1$, $a = 14.990(4)$ Å, $b = 11.737(3)$ Å, $c = 16.417(4)$ Å, $\beta = 112.838(14)°$, $V = 2661.9(11)$ Å^3, $Z = 2$, $r_{calcd} = 1.316$ g cm^{-3}; synchrotron radiation (CCLRC Daresbury Laboratory Station 9.8, silicon monochromator, $\lambda = 0.6875$ Å, $\mu = 0.088$ mm^{-1}, $T = 160(2)$ K. 8047 data (8008 unique, $R_{int} = 0.1706$, $1.30 < \theta < 28.41°$), were collected on a Siemens SMART CCD diffractometer using narrow frames (0.15° in ω) and were corrected semiempirically for absorption and incident beam decay (transmission $0.27-1.00$). The structure was solved by direct methods and refined by full-matrix least squares on F^2 values of all data (G. M.Sheldrick, SHELXTL manual, Siemens Analytical X-ray Instruments, Madison WI, 1994, Version 5) to give $wR = \{\sum[w(F_o^2 - F_c^2)^2]/\sum[w(F_o^2)^2]\}^{1/2} = 0.5073$, conventional $R = 0.2223$ for F values of 7941 reflections with $F_o^2 > 2\sigma(F_o^2)$, $S = 1.202$ for 590 parameters. Isotropic H atoms were constrained; other atoms were refined anisotropically except carbon atoms belonging to the thread. Residual electron density extremes were 2.767 and -1.287 Å^{-3}. Apparent crystal twinning complicated the structure determination of **7** and only one crystal out of several examined gave diffraction data of sufficient intensity to allow a structure determination. Despite the rather high R factor and wR value, the results permit an unambiguous determination of connectivity, packing pattern, the spatial relationship between macrocycle and thread, their conformations and the intercomponent hydrogen bonding motifs.

Experimental details for **8** were the same as for **7** except for the following: $C_{67}H_{66}N_6O_9$, $M = 1099.26$, crystal size $0.04 \times 0.1 \times 0.1$ mm, monoclinic $P2_1/a$, $a = 19.3193(4)$ Å, $b = 15.5788(3)$ Å, $c = 20.7414(4)$ Å, $\alpha = 90$, $\beta = 112.8750(10)$, $\gamma = 90°$, $V = 5751.6(2)$ Å^3, $Z = 4$, $r_{calcd} = 1.269$ g cm^{-3}; synchrotron radiation (CCLRC Daresbury Laboratory Station 9.8, silicon monochromator, $\lambda = 0.6874$ Å), $\mu = 0.085$ mm^{-1}, $T = 160(2)$ K. 34016 data (12600 unique, $R_{int} = 0.0685$, $\theta < 27.22°$) were collected on a Siemens SMART CCD diffractometer using narrow frames (0.3° in ω), and were corrected semiempirically for absorption and incident beam decay (transmission $0.54-1.00$). The structure was solved and refined as described above for **7** to give $wR = \{\sum[w(F_o^2 - F_c^2)^2]/\sum[w(F_o^2)^2]\}^{1/2} = 0.1412$, conventional $R = 0.0645$ for F values of 12600 reflections with $F_o^2 > 2\sigma(F_o^2)$, $S = 0.941$ for 760 parameters. Residual electron density extremes were 0.907 and -0.346 Å^{-3}.

Crystallographic data for both **7** and **8** (excluding structure factors) have been deposited with the Cambridge Crystallographic Data Centre as supplementary publication numbers CCDC-179-101849 (**7**) and CCDC-179-101321 (**8**). Copies of the data can be obtained free of charge on application to The Director, CCDC, 12 Union Road, Cambridge CB2 1EZ, UK (fax: Int. code + (1223)336-033; e-mail: teched@chemcrys.cam.ac.uk).

Supporting Information Available: Tables of crystal data, structure solution and refinement, atomic coordinates, bond lengths and angles, and anisotropic thermal parameter for **7** and **8** (PDF). See any current masthead page for ordering and Web access instructions. This material is available free of charge via the Internet at http://pubs.acs.org.

JA9841310